Gas permeability of polyethylene/poly(ethylene–propylene) semicrystalline diblock copolymers

Peter Kofinas and Robert E. Cohen*†
Department of Materials Science and Engineering and † Department of Chemical Engineering, Massachusetts Institute of Technology, 77 Massachusetts Avenue, Cambridge, MA 02139, USA

and Adel F. Halasa
The Goodyear Tire and Rubber Company, Research Division, 142 Goodyear Boulevard, Akron, OH 44305-0001, USA
(Received 19 April 1993; revised 26 July 1993)

Gas permeability coefficients for several gases (He, CO_2, CH_4, O_2 and N_2) were measured at 25°C in a series of semicrystalline diblock copolymers of polyethylene/poly(ethylene–propylene). A simple model is presented describing the gas transport in these polymer systems. It predicts the permeability of a randomly oriented spherulitic diblock specimen from the values of the permeability coefficients of the individual lamellar regions of the copolymer. Model predictions were in excellent agreement with the experimental data. The upper bound (lamellae aligned in parallel with respect to the permeation direction) and lower bound (series lamellar alignment) models were calculated and compared to a limited amount of corresponding experimental data on oriented specimens.

(Keywords: gas permeability; diblock copolymers; model)

INTRODUCTION

The use of polymers in gas permeation applications is increasing[1,2]. Control over gas transport is essential to the development of polymer membranes for gas separation and barrier material applications. These goals can be achieved with heterogeneous polymer systems, which can be used to design membranes having the structural characteristics of one component and the permeability characteristics of the other. For the case of heterogeneous block copolymers, the features in these systems that affect gas transport are the size, shape and orientation of the microphase separated morphology, the high internal surface-to-volume ratio, and the diffuse interfacial regions.

In previous investigations from this laboratory on gas permeability (P) of a polystyrene (PS)–polybutadiene (PB) block copolymer with a lamellar morphology, alternating lamellae of PS and PB were either misordered[3], aligned in parallel (high P)[4], or in series (low P)[5] with respect to the permeation direction. A simple model was proposed to describe gas transport in this polymer system[3].

In the present study we examine the permeation of various gases through a series of diblock copolymers having crystalline quasi-polyethylene (E) blocks and amorphous poly(ethylene–propylene) (EP) blocks. Mechanical properties of E/EP diblocks and triblocks have been reported[6,7], and some work has been done to characterize the morphology on the length scale of microdomains[7,8]. However, there has been no study of gas transport through these materials. We will demonstrate that the same simple model that described the permeation of gases through the PS/PB system also applies to the E/EP polymers, even though the crystallization of the E blocks provides added degrees of morphological complexity in the E/EP materials.

EXPERIMENTAL

The E/EP block copolymers were synthesized by hydrogenation of 1,4-polybutadiene/1,4-polyisoprene (PI) block copolymers. The butadiene block consists of 10% 1,2-, 35% *trans*-1,4- and 55% *cis*-1,4-PB, while the isoprene block contains 93% *cis*-1,4- and 7% 3,4-PI. The catalytic hydrogenation procedure is described in detail elsewhere[9,10]. Hydrogenated butadiene thus resembles low-density polyethylene (E), and hydrogenated isoprene is essentially perfectly alternating ethylene propylene rubber (EP). PI of molecular weight 100000 was also hydrogenated to produce EP homopolymer. The molecular weights of the E/EP diblocks are listed in *Table 1*. They were determined from g.p.c. measurements on the polydiene precursors (first block and diblock), from knowledge of reactor stoichiometry and conversion, and from a previous demonstration[9] that little or no degradation occurs during the hydrogenation reactions. E/EP films for permeation measurements were prepared by compression moulding at 190°C, by means of a hydraulic press. Prior to permeation measurements, the compression moulded films were annealed under vacuum

* To whom correspondence should be addressed

0032-3861/94/06/1229–07

Table 1 Characterization of E/EP specimens

Sample	$M \times 10^{-3}$ (g mol^{-1})	
	E	EP
E/EP 30/70	30	70
E/EP 50/50	50	50
E/EP 60/40	60	40
E/EP 70/30	70	30
E/EP 60/120	60	120
E/EP 100/100	100	100
E/EP 120/80	120	80
EP 100	0	100

at 120°C for 2 days to minimize any orientation induced by the initial moulding in the press. The melting points of the series of E/EP diblocks were all between 99 and 103°C, as determined by d.s.c.

The E/EP 50/50 diblock was also subjected to plane strain compression at 190°C up to compression ratios of 11. The compressed specimens were slow-cooled under load, followed by load release. Plane strain compression above the melting point of the E block has been determined to produce a morphology where the lamellae are aligned in parallel to the direction of the applied load[11], thereby yielding a film sample in which gas permeation occurs along lamellae aligned in parallel.

The changes in lamellae due to deformation were studied by means of small-angle X-ray scattering (SAXS). The SAXS measurements were performed on a computer-controlled system consisting of a Nicolet two-dimensional position-sensitive detector associated with a Rigaku rotating-anode generator operating at 40 kV and 30 mA and providing CuKα radiation. The primary beam was collimated by two Ni mirrors. In this way the X-ray beam could be effectively focused onto a beam stop with a very fine size without losing much intensity. The specimen-to-detector distance was 2.5 m, and the scattered beam path between the specimen and the detector was enclosed by an Al tube filled with helium gas in order to minimize the background scattering. The specimen-to-detector distance was reduced to 10 cm when performing experiments on crystallite orientation.

A separate Rigaku wide-angle X-ray diffractometer with a rotating anode source was employed throughout the work. The CuKα radiation generated at 50 kV and 60 mA was filtered by electronic filtering and a thin-film Ni filter. X-ray diffraction data were collected by means of a Micro VAX computer running under DMAXB Rigaku-USA software. The slit system that was used allowed for collection of the diffracted beam with a divergence angle of less than 0.3°.

The gases used in this study differed in size and shape: He, CO_2, CH_4, O_2 and N_2. The purities of all gases were in excess of 99.99%. Gas permeability coefficients (P) were determined from steady-state measurements using a variable volume permeation apparatus[12]. All measurements were carried out at 25°C, keeping a pressure difference of 10.5 psig (72.4 kPa) across the sample films.

RESULTS

Figure 1 shows the d.s.c. curve for the E/EP 30/70 specimen. The peak occurring at 99°C is the nominal melting point of E in this sample. The broad melting curve indicates the presence of a wide distribution of crystal sizes and perfection. A polarized light micrograph of a thin film of E/EP diblocks, which was heated above 100°C in the optical microscope and then cooled to room temperature, is presented in *Figure 2*. Crystallization occurs almost instantaneously as the polymers are cooled below their melting point; varying the thermal history does not greatly affect the degree of crystallinity. All diblocks exhibit spherulitic morphology when crystallized from the melt, even in the sample containing as little as 30% E, indicating that lamellae predominate over the entire composition range examined here.

Figure 3 shows a two-dimensional wide-angle X-ray diffraction (WAXD) pattern, and the corresponding radial average plot of intensity, $I(Q)$, *versus* scattering vector magnitude, Q, for a typical misoriented sample used in the permeation experiments ($Q = (4\pi/\lambda)\sin\theta$ and the scattering angle is 2θ). The pattern has the shape of concentric rings, with the intensity being uniform along all azimuthal angles, as expected from an undeformed spherulitic specimen. The crystalline structure of the E/EP polymers is observed with better resolution from

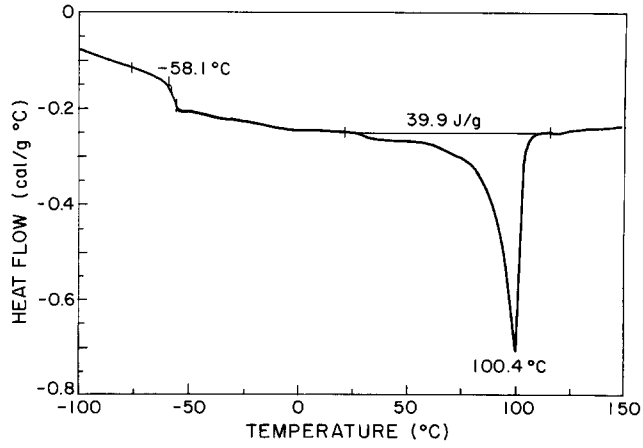

Figure 1 D.s.c. scan for E/EP 30/70

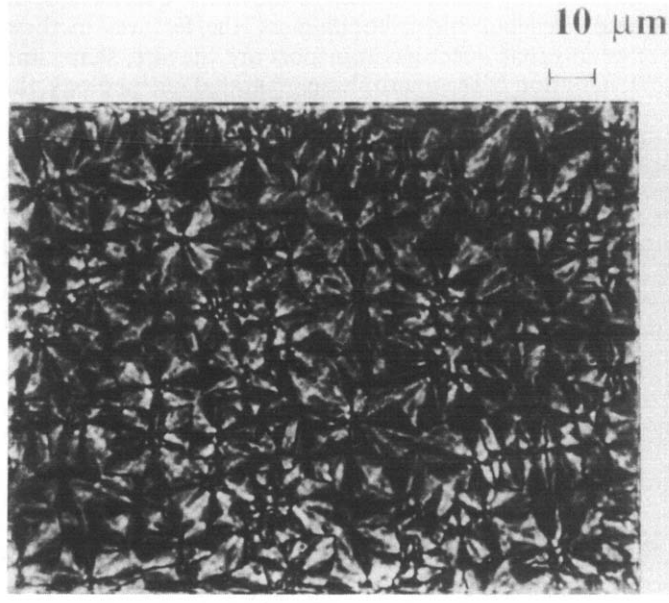

Figure 2 Optical micrograph of E/EP 60/40 crystallized from the melt

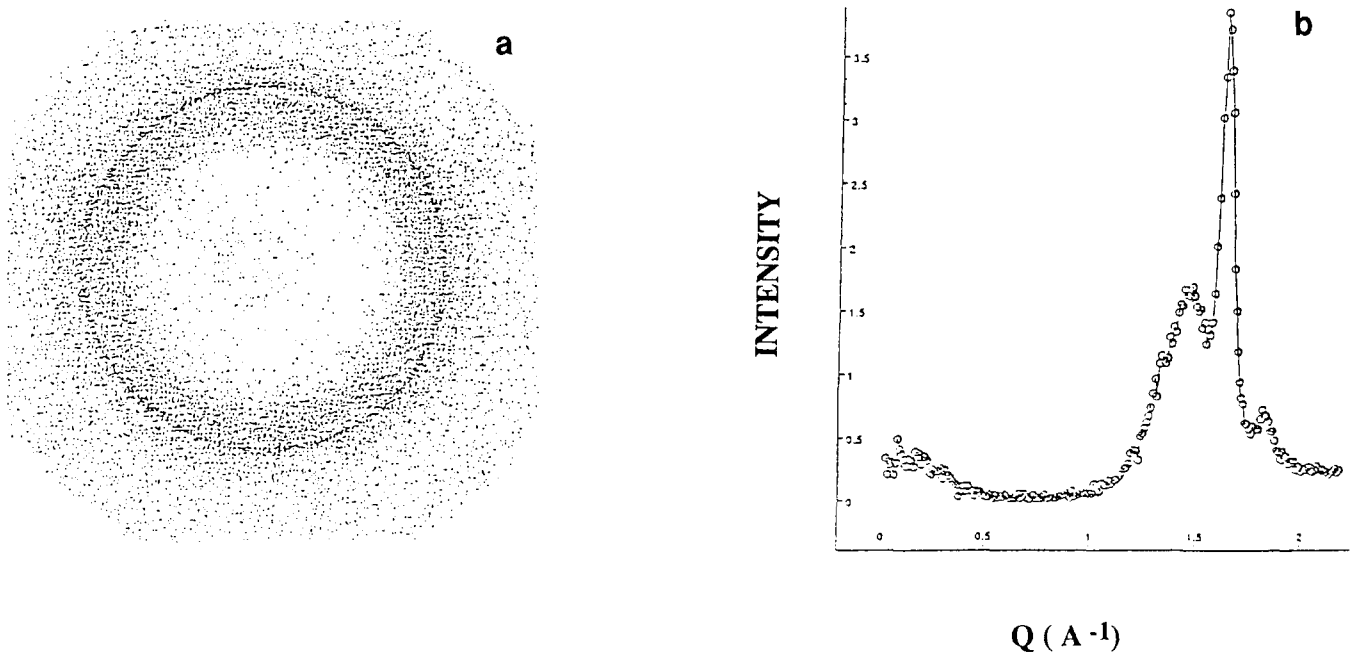

Figure 3 (a) Two-dimensional WAXD pattern and (b) corresponding radial average for E/EP 50/50

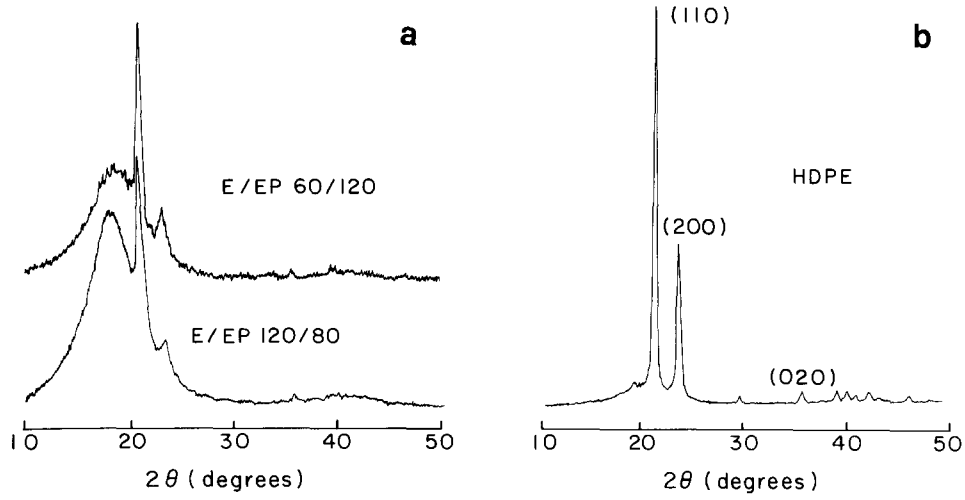

Figure 4 WAXD 2θ scans: (a) E/EP 60/120, E/EP 120/80 and (b) HDPE

a 2θ scan in the wide-angle diffractometer. As shown in *Figure 4*, which compares the 2θ scans of a high-density polyethylene (HDPE) to two of the E/EP diblocks, the diffraction peaks observed in the E/EP copolymers correspond to the (110), (200) and (020) diffraction planes of the orthorhombic unit cell of polyethylene[13]. In addition to the HDPE diffraction planes, a broad amorphous halo centred around $2\theta = 20°$ is observed. The intensity of the amorphous halo increases as the amorphous block content in the diblock increases (compare *Figures 4a* and *4b*).

The permeation results for the entire series of misoriented spherulitic diblocks as well as for the EP homopolymer are shown in *Table 2*. As expected, these materials have rather low permeabilities, which decrease with increasing crystallinity (increasing amount of E block). From the comparison of the P values for specimens containing the same percentage of E in the EP diblock (E/EP 50/50 and E/EP 100/100, E/EP 120/80 and E/EP 60/40), it is apparent that the permeability is independent of the total molecular weight of the polymer. The permeability value for the E block lamellae also appears in *Table 2*. These values were not measured directly but were obtained from extrapolations of the fits (non-linear fitting routine FMINS of the commercially available software package MATLAB) to the permeability data for the series of diblocks of varying E-block content (*Figure 5*). Although the E lamellae contain internal structural complexities such as chain folding and amorphous fractions, we group all of these details into a quasi-homogeneous material parameter P_E, the effective permeability of E-like material in the E domains of the E/EP diblocks. Justification of this simplification will be demonstrated below.

The SAXS patterns of the E/EP 50/50 specimen subjected to plane strain compression at 150 and at 80°C is shown in *Figure 6*, accompanied by a sketch of the lamellar orientation. The specimen orientation during

Table 2 Permeability coefficients (P, in barrers) for spherulitic specimens at 25°C

Gas	EP 100	E/EP									
		30/70	60/120	50/50	100/100	120/80	60/40	70/30	E[a]	E[b]	LDPE[c]
He	78.1	33.5	32.0	17.6	18.6	16.3	17.2	13.6	6.5	15.7	4.9
CH_4	29.2	13.5	16.4	9.9	8.8	14.5	10.6	8.7	6.9	13.0	2.9
CO_2	117.0	72.7	51.8	46.7	44.2	39.5	38.4	36.6	25.5	48.4	12.7
N_2	22.3	3.9		3.4	3.9	3.7	2.2	1.9			
O_2	37.5	16.5	13.4	8.9	10.6	11.5	11.2	7.8	6.9	11.3	2.9

[a] Value for E extrapolated from fit to data
[b] Hydrogenated butadiene, crystallinity 29%, $\rho = 0.894\ g\ cm^{-3}$
[c] LDPE, $\rho = 0.914\ g\ cm^{-3}$

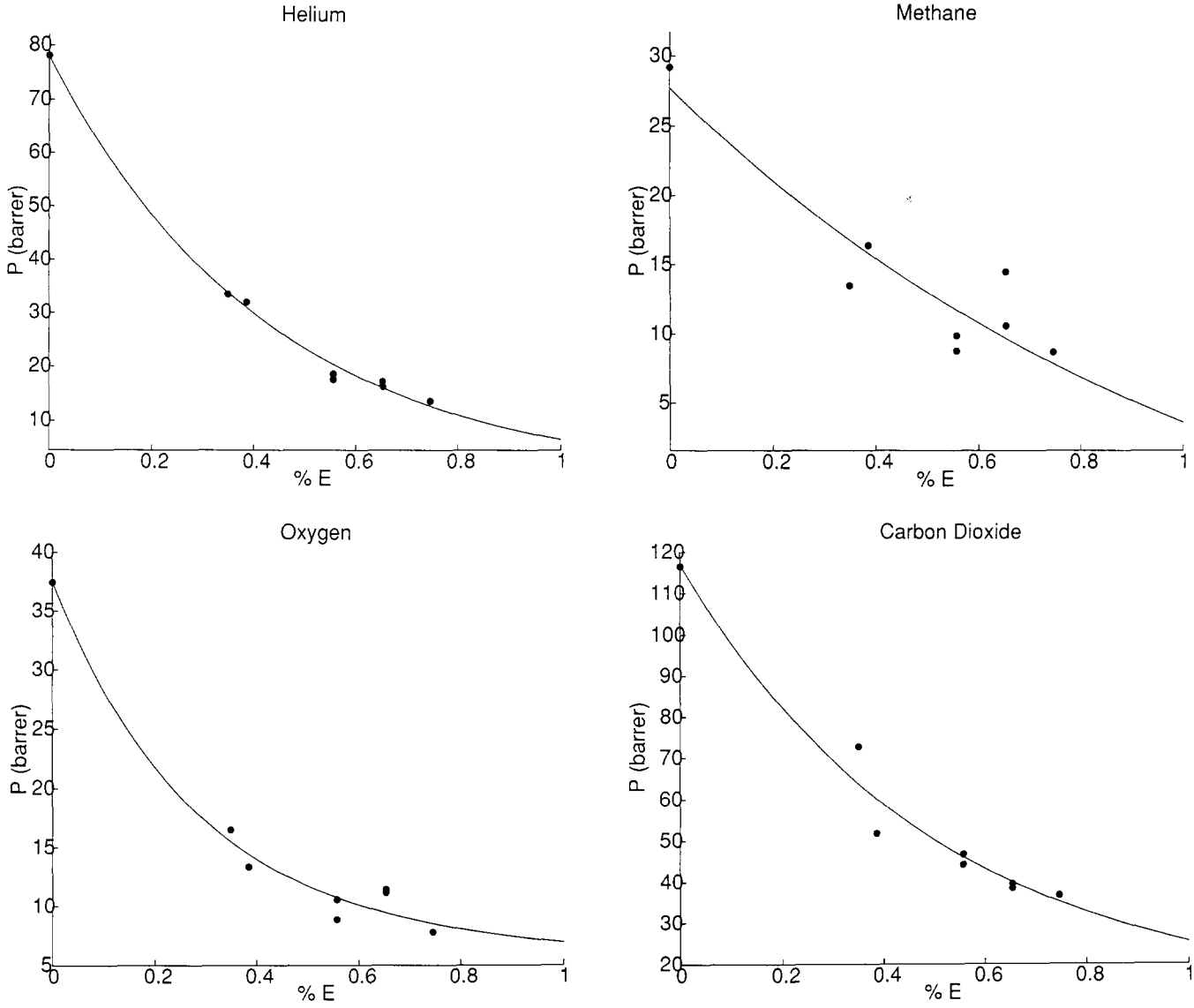

Figure 5 Permeability *versus* E-block content for spherulitic specimens

collection of the X-ray spectra is indicated with respect to the principal directions of deformation, i.e. the compression direction (CD), the free (or flow) direction (FD) and the loading direction (LD). As seen from the SAXS pattern, the morphology changes from parallel lamellar with respect to the permeation direction (LD) when the specimen is textured above its melting point, to series lamellar below the melt. The permeation of the specimen with the lamellae aligned in parallel with respect to the permeation direction (P_{par}) was measured and is reported in *Table 3*. We were unsuccessful in preparing a large enough pinhole and crack-free specimen of the series lamellar type for gas transport measurements. There is, however, indication[14] that the series lamellar morphology could also be achieved through texturing above the melting point of the E block, using large strain

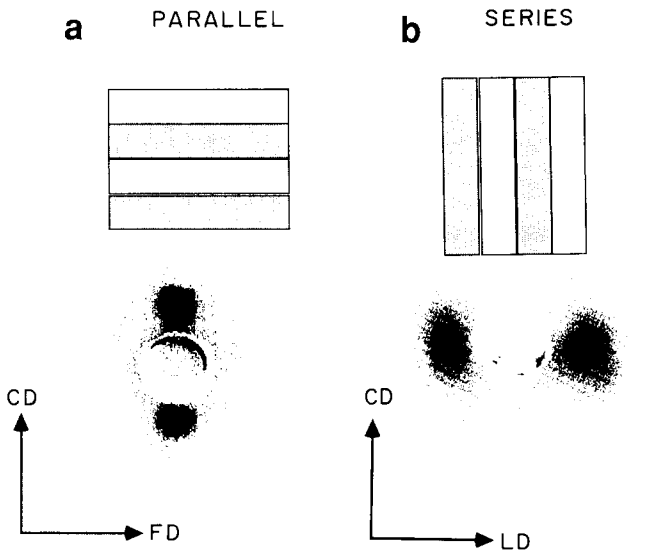

Figure 6 SAXS of E/EP 50/50 oriented above (a) and below (b) the melting point via plane strain compression. In the permeation tests gas flow is always along LD

Table 3 Model prediction of P (in barrers) in spherulitic specimens at 25°C from the P values of the individual block species

	E/EP				
Gas	30/70	60/120	50/50 100/100	60/40 120/80	70/30
He	29.0	27.3	20.5	17.2	14.1
CH_4	16.0	15.3	12.4	10.9	9.7
CO_2	62.1	59.2	47.5	41.8	36.8
O_2	18.6	17.7	13.9	12.2	10.6

dynamic shear at low shear rates. A series specimen thus fabricated should be suitable for permeation measurements. Ongoing research includes the study[11] of the parameters favouring the presence of the series *versus* the parallel lamellar morphology in a deformed block copolymer specimen.

DISCUSSION

Gas molecules are generally taken to be insoluble in polymer crystallites and are therefore unable to permeate through them[15]. Thus, gas permeation in semicrystalline polymers is essentially confined to the amorphous regions. The crystallites reduce the permeability by decreasing the volume of polymer available for penetrant solution and by constraining the transport along irregular tortuous paths between the crystallites. The reduction in permeability (P), which is the product of the effective diffusion (D) and solubility (S) coefficients, will thus be proportional to the volume fraction of the crystalline phase[16] when all samples have a random misoriented morphology.

The morphology of the E block in any phase-separated E/EP diblock copolymer differs from the morphology of a homopolymer of E, because of the topological constraint imposed at the junction between the two blocks in the diblock copolymer. Since even the slightest morphological differences between two materials can result in big variations in their gas permeability characteristics, P of an E homopolymer for a specific gas does not correspond to P of an E block in the E/EP diblock. The permeability value for the E block was therefore extrapolated from the experimental data, rather than measured from an actual specimen; values of the E-block permeability appear in *Table 2*. For all gases, these values fall between the permeability values for a typical low density polyethylene (LDPE) ($\rho = 0.914\ g\ cm^{-3}$)[17] and of a hydrogenated PB ($\rho = 0.894\ g\ cm^{-3}$)[17], as shown in *Table 2*. On the other hand, the EP homopolymer is considered to be 100% amorphous, hence in this case P of the EP block in an E/EP copolymer can be taken to be the same as P of the EP homopolymer, which was determined experimentally.

The effect of microphase orientation on gas permeability is significant. Permeability coefficients for a film whose microdomains are oriented normal to the film surface (parallel to the permeation direction), are much higher than for a film having its microdomains oriented in the same plane as the film surface (in series with respect to the permeation direction)[4]. The resulting expressions for parallel and series laminates for the case of the E/EP diblock copolymers are:

$$P_{par} = P_E v_E + P_{EP} v_{EP} \quad (1)$$

$$P_{ser} = \frac{P_E P_{EP}}{P_E v_{EP} + P_{EP} v_E} \quad (2)$$

where P_E, P_{EP} = permeability coefficient for the E and EP blocks, respectively, and v represents the volume fraction.

The values of the effective permeabilities of the E (fit) and EP (measured) blocks were used in the construction of a model predicting gas transport behaviour in misoriented heterogeneous polymer systems. This 'random column model' has already been successfully applied to a PS–PB diblock copolymer system[3]. We now examine its validity for diblock copolymers which contain one block that is crystallizable.

The morphology of the sample is modelled as columns of cubical cells, with each column extending directly from one surface of the film to the other. Each cell contains alternating parallel lamellae that possess a direction of orientation defined[3] by a random angle θ. A periodic boundary condition is imposed at the left and right sides of the cell so that any gas that 'leaves' through either side of the cell as it travels parallel to the orientation direction re-enters at the opposing side. It is assumed that the permeating species will preferentially diffuse parallel to the lamellar orientation in each cell. The effective permeability for each cell can be defined as the permeability for a parallel lamellar system, divided by a path length or tortuosity factor τ, which will change from cell to cell. The tortuosity accounts for the fact that a lamellar alignment angle θ other than zero increases the path length that a diffusing molecule must travel in order to reach the cell $i+1$ below:

$$P_i = \frac{P_{par}}{\tau_i} \quad (3)$$

$$\tau_i = \frac{1}{\cos \theta_i} \quad (4)$$

An important constraint imposed on P_i is that a cell's permeability coefficient cannot be lower than that given by the series representation, equation (2). If the tortuosity of a cell is so large that the permeability calculated by

equation (3) is lower than that for the series model, the series value is assigned as the permeability for that cell. The diffusing species is thus allowed to 'choose' the faster of the two modes through any cell, and the effective permeability of the entire column is obtained with the summation *in series* of the individual P_i for each cell:

$$\frac{1}{P_{\text{eff}}} = \frac{1}{N}\sum_{i=1}^{N}\frac{1}{P_i} \tag{5}$$

where N = number of cells in the column.

A computer simulation obtaining the average P of 10000 columns with $N = 10000$ cells each has been carried out for He, CO_2, CH_4 and O_2 for all compositions. The number of columns, and cells in each column, were chosen to be large enough so that the variations in the permeability coefficient calculated from each run would be minimized. The standard deviation in the P values calculated from each simulation was thus reduced to ± 0.1 barrers. The values of θ_i for each cell were calculated using a random number generator. *Figure 7* shows a plot of P *versus* number of cells and columns. It is evident that above $N \times N = 1000 \times 1000$ there is no variation in the P values; thus the value of 10000×10000 chosen for the simulation is more than adequate to describe a purely random specimen.

Table 4 E/EP 50/50 model prediction of P_{par} (in barrers) compared to experimental measurements

Gas	P_{par} (exp)	P_{par} (model)
He	37.2	38.3
CH_4	15.6	16.8
CO_2	63.3	66.1
O_2	20.5	20.9
N_2	11.5	12.5

The predictions of the random column model for the permeability coefficients of a randomly oriented sample are shown in *Table 4*. The agreement between experiment (*Table 2*) and model (*Table 4*) is quite good. The values for P_{par} calculated from the model for the E/EP 50/50 polymer, are compared in *Table 3* to experimental measurements of P_{par} in the plane strain compressed sample. The parallel model (equation (1)) is in very good agreement with the experimentally measured value of P_{par}. The model slightly overpredicts the experimental value for all gases, since we cannot expect to construct experimentally a specimen with all of its lamellae being perfectly oriented parallel to the permeation direction; there will always be some tortuosity in the lamellae, which will reduce the effective permeability of the specimen. We note, however, that this level of agreement between the upper bound model and the near-parallel experimental material suggests that the input (extrapolated) values of P_E for each gas represent a very good approximation to the experimentally inaccessible permeation behaviour of the semicrystalline E-block domains of the various diblock copolymers. The predictions of the respective models for the parallel and series morphologies for each diblock specimen studied are presented in *Table 5*; this is an indication of the upper and lower bounds to gas permeability that can be achieved with each specimen for the gases studied.

The good agreement between model and measurement also serves to justify our simplification of permeation in the crystallizable E lamellae as described by a single parameter P_E. The fact that the random column model works well for a series of gases, whose ratio of permeabilities EP to E varies from 4 to 12, demonstrates convincingly its ability to simulate the gas transport behaviour of these semicrystalline block copolymers over a wide range of permeabilities.

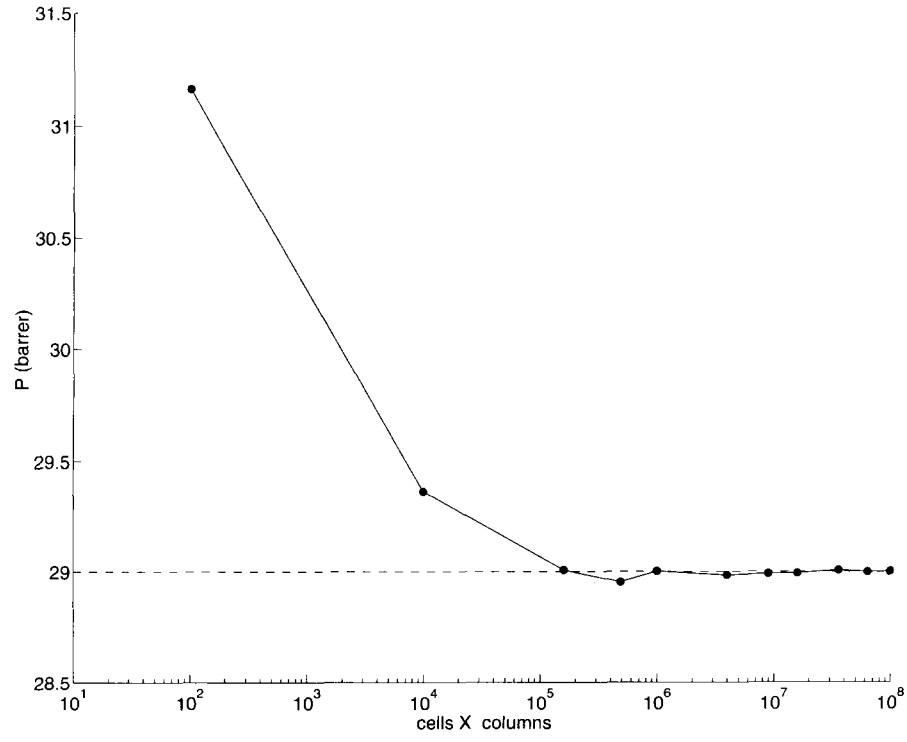

Figure 7 Model predictions of permeability *versus* number of cells and number of columns; He in E/EP 30/70

Table 5 Model predictions of P_{par} and P_{ser} (in barrers)

	E/EP									
	30/70		60/120		50/50 100/100		60/40 120/80		70/30	
Gas	P_{par}	P_{ser}	P_{par}	P_{ser}	P_{par}	P_{ser}	P_{par}	P_{ser}	P_{par}	P_{ser}
He	53.1	16.1	50.5	14.9	38.3	10.9	31.4	9.5	24.8	8.4
CH_4	21.4	13.7	20.6	13.0	16.8	10.4	14.7	9.4	12.6	8.6
CO_2	85.1	51.9	81.8	49.1	66.2	39.0	57.3	35.0	48.8	31.8
O_2	26.8	14.7	25.7	13.9	20.5	10.8	17.6	9.6	14.7	8.7

SUMMARY

A simple model of gas permeation in misoriented lamellar materials successfully describes the permeation behaviour for a series of spherulitic E/EP diblock copolymers with a wide range of compositions. The model assumes that the majority of the transport takes place along the more conductive, amorphous EP lamella but recognizes the smaller, but non-zero, permeability of the semicrystalline E domains. The observed lowering of the permeability of the copolymer by the presence of these semicrystalline E regions is accounted for in the model through considerations of its volume fraction and through an effective tortuosity which is introduced into the materials. Values of P_{EP} could be determined directly via gas permeation measurements on the corresponding EP amorphous homopolymer; however, the permeation behaviour of the semicrystalline E domains could not be obtained in a similar fashion because their internal structural details[18] are different from the corresponding E homopolymer, due to the topological constraint imposed at the junction of the E and EP blocks in the E/EP diblock copolymer. Therefore P_E values were obtained by extrapolation of permeation data for a series of copolymers of varying E-block content.

The excellent agreement between the random column model and experiments in the E/EP materials suggests that permeabilities of other spherulitic semicrystalline diblock copolymers can be anticipated without the need for synthesizing every candidate system under consideration. The upper and lower bounds (parallel and series) models represent the limiting cases for high throughput or good barrier membranes, respectively. The oxygen permeability of butyl rubber, a barrier elastomer, is 2.1 barrers[19]. This value is not dramatically lower than the predicted value of 8.7 barrers for the series E/EP 70/30 material (*Table 5*), thus suggesting possible uses of the E/EP diblocks as barrier materials in certain applications. We also note that the superficial mechanical properties (stiffness *versus* flexibility) depend greatly on the volume fraction composition of the E/EP diblocks, which represents another possible degree of freedom in membrane design using these materials.

In our work to date we have examined only diblock copolymer structures. Ongoing research includes studies of tri- and tetrablock copolymers of E/EP covering a wide range of composition and molecular weight.

ACKNOWLEDGEMENTS

This research has been supported by the Office of Naval Research and the Goodyear Tire and Rubber Company. Assistance with gas permeability measurements was provided by Ana I. Laplaza, with support from the MIT Undergraduate Research Opportunities Program.

REFERENCES

1 Haggin, J. *Chem. Eng. News* 1988, **66** (23), 7
2 Comyn, J. (Ed.) 'Polymer Permeability', Elsevier Applied Science, London, 1985
3 Csernica, J., Baddour, R. F. and Cohen, R. E. *Macromolecules* 1989, **22**, 1493
4 Csernica J., Baddour, R. F. and Cohen, R. E. *Macromolecules* 1987, **20**, 2468
5 Csernica, J., Baddour, R. F. and Cohen, R. E. *Macromolecules* 1990, **23**, 1429
6 Mohajer, Y., Wilkes, G. L., Wang, J. E. and McGrath, J. E. *Polymer* 1982, **23**, 1523
7 Seguela, R. and Prud'homme, J. *Polymer* 1989, **30**, 1446
8 Rangarajan, P., Register, R. A. and Fetters, L. J. *Am. Chem. Soc. Div. Polym. Chem. Polym. Prepr.* 1992, **33** (2), 424
9 Halasa, A. F. US Patent 3 872 072
10 Cohen, R. E., Cheng, P.-L., Douzinas, K., Kofinas, P. and Berney, C. V. *Macromolecules* 1990, **23**, 324
11 Kofinas, P., Cohen, R. E. and Halasa, A. F. in preparation
12 ASTM D-1434, American Society for Testing and Materials, Philadelphia, 1984
13 Spruiell, J. E. and Clark, E. S. 'Methods of Experimental Physics', Academic Press, New York, 1980, Vol. 16B, Ch. 6
14 Koppi, K. A., Tirrell, M., Bates, F. S., Almdal, K. and Colby, R. H. *J. Phys. II* 1993, **2** (11), 1941
15 Michaels, A. S., Vieth, W. R. and Barrie, J. A. *J. Appl. Phys.* 1963, **34** (1), 1
16 Mohr, J. M. and Paul, D. R. *J. Appl. Polym. Sci.* 1991, **42**, 1711
17 Pauly, S. in 'Polymer Handbook' 3rd Edn (Eds J. Brandrup and E. H. Immergut), Wiley, New York, 1989
18 Douzinas, K. C. and Cohen, R. E. *Macromolecules* 1992, **25**, 5030
19 van Amerongen, G. J. *J. Appl. Phys.* 1946, **17**, 972